On the Numerical Implementation of a Thermomechanical Hyperplasticity Model for Fine-Grained Soils

Golchin, A.; Vardon, Philip J.; Hicks, Michael A.; Coombs, William M.; Pantev, I. A.

DOI
10.1007/978-3-030-64514-4_40

Publication date
2021

Document Version
Final published version

Published in
Challenges and Innovations in Geomechanics - Proceedings of the 16th International Conference of IACMAG - Volume 1

Citation (APA)
Golchin, A., Vardon, P. J., Hicks, M. A., Coombs, W. M., & Pantev, I. A. (2021). On the Numerical Implementation of a Thermomechanical Hyperplasticity Model for Fine-Grained Soils. In M. Barla, A. Di Donna, & D. Sterpi (Eds.), *Challenges and Innovations in Geomechanics - Proceedings of the 16th International Conference of IACMAG - Volume 1* (pp. 422-429). (Lecture Notes in Civil Engineering; Vol. 125). Springer. https://doi.org/10.1007/978-3-030-64514-4_40

Important note
To cite this publication, please use the final published version (if applicable).
Please check the document version above.

On the Numerical Implementation of a Thermomechanical Hyperplasticity Model for Fine-Grained Soils

A. Golchin[1(✉)], Philip J. Vardon[1], Michael A. Hicks[1], William M. Coombs[2], and I.A. Pantev[1]

[1] Section of Geo-Engineering, Delft University of Technology, Stevinweg 1, 2628 CN Delft, The Netherlands
A.Golchin@tudelft.nl
[2] Department of Engineering, Durham University, Lower Mountjoy, South Road, Durham DH1 3LE, UK

Abstract. The numerical implementation of a recently developed thermomechanical constitutive model for fine-grained soils based on hyperelasticity-hyperplasticity theory (Golchin et al. 2020), is presented. A new unconventional implicit stress return mapping algorithm, compatible with elasticity derived from Gibbs (complementary) energy potential, in strain invariant space, is designed and the consistent tangent operator for use in boundary value problems (such as in the finite element method) is derived. It is shown that the rate of convergence of the stress integration algorithm is quadratic. The numerical results are in good agreement with available data from thermomechanical element tests found in literature.

Keywords: Gibbs free energy · Hyperplasticity · Implicit integration · Thermomechanical model

1 Introduction

Boundary-value solvers (BVS) allow simulation of complex geometries, material behaviour and loading, efficiently giving results for displacements and forces. The finite element method is one such numerical tool. Constitutive models with sophisticated mathematical formulations have been developed to reproduce the complex behaviour of soils (e.g. elastoplasticity) as accurately as possible. In materials that yield and exhibit nonlinearity, numerical algorithms are needed for BVS.

Recently, Golchin et al. (2020) developed a constitutive model that predicts the thermo-mechanical behaviour of fine-grained soils. These types of constitutive models are essential for simulating and investigating thermal effects on the behaviour of thermo-active structures such as energy-piles, thermal quay walls, pipelines and so on. This model has been developed using the hyperelasticity-hyperplasticity framework proposed by Collins and Houlsby (1997) and ensures satisfaction of thermodynamics principles.

M. Barla et al. (Eds.): IACMAG 2021, LNCE 125, pp. 422–429, 2021.
https://doi.org/10.1007/978-3-030-64514-4_40

Here, the focus is exclusively on the implicit implementation of the constitutive model in the finite element method (or any boundary-value solver). This generally requires the material constitutive equations (stress–strain relationship) to be integrated over time steps (local integration) (Anandarajah 2010; Borja 2013). These schemes are broadly categorised as explicit, implicit or combined (Scalet and Auricchio 2018). Both former approaches can provide accurate solutions; implicit approaches are stable at bigger time steps, whereas the explicit approach requires small time steps to remain stable (Scalet and Auricchio 2018). Moreover, the consistency condition is imposed in the implicit approach to ensure that the stress remains on the yield surface under elastic–plastic behaviour.

"Elastic predictor-plastic corrector" algorithms incorporate the implicit scheme and have been developed and used in past decades (Anandarajah 2010; Borja 2013; Coombs et al. 2013; Coombs and Crouch 2011). As can be inferred by their name, these algorithms comprise two steps: in the first step an elastic prediction (trial strain or stress) is applied; in the next step, if the trial state is not possible, i.e. exceeds a yield criterion, it triggers plasticity, so that the internal variables then evolve and the stress state is returned back onto the yield surface.

Implicit implementation of hyperelastic-plastic models, with elasticity derived from Helmholtz free energy, for both isothermal and non-isothermal conditions, have been addressed in the works of, for example, Anandarajah (2010), Borja (2013), Coombs and Crouch (2011), and Semnani et al. (2016). In this work, a complementary energy potential (Gibbs free energy potential) is defined to determine the nonlinear stress-dependent thermo-elasticity of soils. As a result, an unconventional approach for stress integration is required in order for the model to be used in boundary-value solvers.

2 Constitutive Equations

The constitutive equations are derived based on the hyperplasticity framework. Only the necessary equations for numerical implementation in a finite element scheme are presented here. The complete set of equations are described in Golchin et al. (2020).

Within hyperplasticity-theory the definition of two scalar potentials, namely energy and dissipation potentials, are sufficient to derive the entire constitutive equations for the behaviour of materials (Collins and Houlsby 1997). The model adopts a Gibbs-type free energy potential, which results in expressions that define the elastic behaviour of the soil by stress terms. The energy potential is defined as:

$$\begin{aligned} E\left(p,q,\varepsilon_v^p,\varepsilon_s^p,T\right) &= E_1(p,q) - p\varepsilon_v^p - q\varepsilon_s^p - 3\alpha^* p(T-T_0) \\ E_1(p,q) &= -\kappa p\left(\ln\left(p/p_{ref}\right) - 1\right) - \left(q^2/6\overline{G}p\right) \end{aligned} \tag{1}$$

where $p = tr(\boldsymbol{\sigma})/3$ (kPa) and $q = (3/2\ \mathbf{s}{:}\mathbf{s})^{1/2}$ (kPa) are the mean effective and deviatoric stress, respectively; $\boldsymbol{\sigma}$ and $\mathbf{s} = \boldsymbol{\sigma} - tr(\boldsymbol{\sigma})/3{:}\mathbf{1}$ are the effective stress and deviatoric stress tensors, respectively; $\mathbf{1}$ is the identity tensor; $\varepsilon_v{}^p = tr(\boldsymbol{\varepsilon}^{\mathbf{p}})$ and $\varepsilon_s{}^p = (2/3\ \mathbf{e}^{\mathbf{p}}{:}\mathbf{e}^{\mathbf{p}})^{1/2}$ are plastic volumetric and plastic deviatoric strain invariants, respectively; $\mathbf{e}^{\mathbf{p}} = \boldsymbol{\varepsilon}^{\mathbf{p}} - tr(\boldsymbol{\varepsilon}^{\mathbf{p}})/3{:}\mathbf{1}$, $\boldsymbol{\varepsilon}^{\mathbf{p}}$ and $\mathbf{e}^{\mathbf{p}}$ are plastic strain and plastic deviatoric strain tensors, respectively; α^* is

the linear thermal expansion coefficient of the soil skeleton; T and T_0 are the current and initial absolute temperatures (K), respectively; p_{ref} (kPa) is the reference pressure (normally 1 kPa); $\overline{G}$ is a material constant related to the elastic shear modulus, and κ is the elastic compressibility index, as used in models such as Modified Cam Clay (MCC).

The total strain tensor $\boldsymbol{\varepsilon}$ is determined as the first derivative of the complementary energy potential (E) with respect to stress:

$$\boldsymbol{\varepsilon} = -\partial E/\partial \boldsymbol{\sigma} = \boldsymbol{\varepsilon}^e + \boldsymbol{\varepsilon}^{Therm} + \boldsymbol{\varepsilon}^p,\ \boldsymbol{\varepsilon}^e = -\partial E_1/\partial \boldsymbol{\sigma}, \boldsymbol{\varepsilon}^{Therm} = \alpha^*(T - T_0)\mathbf{1} \tag{2}$$

where strains with superscripts e, *Therm* and p stand for elastic, thermo-elastic and plastic components of the total strain, respectively. Time differentiation of Eq. (2) results in rate form of the total strain tensor (the dot represents the rate):

$$\dot{\boldsymbol{\varepsilon}} = \dot{\boldsymbol{\varepsilon}}^e + \dot{\boldsymbol{\varepsilon}}^{Therm} + \dot{\boldsymbol{\varepsilon}}^p,\ \dot{\boldsymbol{\varepsilon}}^e = -\partial^2 E_1/\partial \boldsymbol{\sigma}^2 : \dot{\sigma},\ \dot{\boldsymbol{\varepsilon}}^{Therm} = \alpha^* \dot{T}\mathbf{1},\ \dot{\boldsymbol{\varepsilon}}^p = \dot{\Lambda}\mathbf{r} \tag{3}$$

$\dot{\Lambda}$ is the plastic multiplier or consistent parameter and $\mathbf{r}$ is the direction of plastic strain or plastic flow tensor (which will be defined later).

For this model, the dissipation potential (d) is defined as:

$$\begin{aligned} &d = C\left(\dot{\varepsilon}_v^p + \beta \dot{\varepsilon}_s^p\right) + \sqrt{A^2\left(\dot{\varepsilon}_v^p + \beta \dot{\varepsilon}_s^p\right)^2 + B^2\left(\dot{\varepsilon}_s^p\right)^2} \\ &A = (1-\gamma)p + (\gamma/2)p_{cT},\ B = M((1-\alpha)p + (\alpha\gamma/2)p_{cT}),\ C = (\gamma/2)p_{cT} \\ &M = M_0 + \pi(T - T_0),\ p_{cT} = p_{ref} e^{\left(\frac{1+e_0}{\lambda-\kappa}\right)\varepsilon_v^p}\ e^{-\mu(T-T_0)} \end{aligned} \tag{4}$$

$\dot{\varepsilon}_v^p$ and $\dot{\varepsilon}_s^p$ are plastic volumetric and deviatoric strain increments, respectively; β represents the inclination level of the yield surface with respect to the p-axis; A, B and C are functions defining the shape of the yield function; α and γ are parameters that affect the shape of the yield surface; M_0 is the critical state stress ratio at ambient temperature; π controls the change of M with temperature variation; p_{cT} is the apparent pre-consolidation pressure; λ is the slope of the normal compression line (NCL) in void ratio, e, versus ln$p$ space; e_0 is the initial void ratio; and μ is the coefficient of thermal softening, defining how the size of the yield surface changes by temperature.

The yield surface, y, and non-associated flow rule (r_p, r_q) can be derived from the dissipation function (see Golchin et al. 2020), and are respectively, defined as:

$$y = (p - C)^2/A^2 + (q - \beta p)^2/B^2 - 1 = 0 \tag{5}$$

$$r_p = 2(p - C)/A^2 - 2\beta(q - \beta p)/B^2;\ r_q = 2(q - \beta p)/B^2 \tag{6}$$

where r_p and r_q are the directions of plastic flow parallel to the p- and q- axes, respectively. The model employs an isotropic hardening rule:

$$\dot{p}_{cT} = \left(\frac{1+e_0}{\lambda-\kappa}\dot{\varepsilon}_v^p - \mu\dot{T}\right)p_{cT} \tag{7}$$

3 Implicit Implementation of Constitutive Equations

A combination of different principles (such as virtual work principle) may be employed to develop finite element equations for a mechanical boundary value problem. The typical final form of the governing equations is (Anandarajah 2010; Borja 2013):

$$\mathbf{Ku} = \mathbf{P} \tag{8}$$

where **K**, **u** and **P** are the global stiffness matrix, the global unknown nodal displacement vector and the global force vector, respectively. For problems involving elastoplastic material behaviour, the global stiffness matrix is dependent on the global displacement **u**, i.e. is nonlinear. As a result, an iterative algorithm, such as Newton–Raphson, is required to solve the global finite element problem (Eq. (8)). The global stiffness matrix **K** is established by assembling the stiffness matrix $\mathbf{k_i}$ of all the elements:

$$\mathbf{K} = \sum_{i=1}^{i=N_E} \mathbf{k_i} = \sum_{i=1}^{i=N_E} \int_{\Omega_i} \mathbf{B^T D_O B} dv \tag{9}$$

where i is the number of the corresponding element; $\sum$ represents the assembly operator; Ω_i is the element i domain and N_E is the number of elements; **B** is the strain–displacement matrix; and $\mathbf{D_O}$ is the consistent tangent operator, defined as:

$$\mathbf{D_O} = \partial\Delta\boldsymbol{\sigma}/\partial\Delta\boldsymbol{\varepsilon} \tag{10}$$

and represents a linearisation of the constitutive relation.

Constitutive relations for elastoplastic materials are mostly developed in rate form:

$$\dot{\sigma} = \mathbf{D}\dot{\varepsilon} \tag{11}$$

where **D** is the elastoplastic continuum tangent. The tangent operator $\mathbf{D_O}$ is different from the continuum tangent **D**. The tangent operator plays a similar role to the continuum tangent, but for a discretised problem. After the system of governing equation (Eq. (8)) is solved, the rate equation (Eq. (11)) needs to be integrated; i.e., an integration procedure of the rate-form constitutive equations (from $\dot{\sigma} = \mathbf{D}\dot{\varepsilon}$) at the Gauss points is required, to ensure all state variables are consistently solved. Any resulting imbalanced forces can be solved via iteration of the solution procedure. An updated tangent operator for the next step then needs to be calculated (depending on the global solution method).

3.1 Stress Integration

Assuming that within a typical time step (t, $t + \Delta t$) the state variables (e.g. stress and strain), hardening variables (e.g. apparent pre-consolidation pressure) and absolute temperature at time t (values at time t are represented by n) ($\boldsymbol{\sigma}_n$, $\boldsymbol{\varepsilon}_n$, p_{cT}^n, T_n) are converged and known, and the strain and temperature increments ($\boldsymbol{\Delta\varepsilon}$, ΔT) are given. Then the state variables at time $t + \Delta t$ (denoted by $n + 1$) ($\boldsymbol{\sigma}_{n+1}$, $\boldsymbol{\varepsilon}_{n+1}$, p_{cT}^{n+1}) must be calculated by an integration scheme. Here, an implicit closed point projection method (CPPM), a sub-class of the elastic predictor-plastic corrector algorithms, is employed to implement the thermo-mechanical constitutive equations.

Appropriate residual equations are defined and minimised using an iterative approach such as the Newton–Raphson method. Stress or strain may be selected to define the first residual equation. For the current model, an unconventional approach is designed in which strain is considered as the state variable to derive the first residual, $\mathbf{R}_1$, and the residual equation is defined by stress terms with an apparent pre-consolidation pressure and plastic multiplier:

$$\mathbf{R}_1\left(\boldsymbol{\sigma}_{n+1}, p_{cT}^{n+1}, \Delta\Lambda\right) = \boldsymbol{\varepsilon}_{n+1}^{e} - \boldsymbol{\varepsilon}^{e,trial} + \Delta\boldsymbol{\varepsilon}_{n+1}^{p} = -\partial E_1/\partial\boldsymbol{\sigma}_{n+1} - \boldsymbol{\varepsilon}^{e,trial} + \Delta\Lambda\mathbf{r} \tag{12}$$

where $\boldsymbol{\varepsilon}^{\mathrm{e,trial}}$ is the trial elastic strain defined as:

$$\boldsymbol{\varepsilon}^{e,trial} = \boldsymbol{\varepsilon}_n^{e} + \Delta\boldsymbol{\varepsilon} - \Delta\boldsymbol{\varepsilon}^{Therm} \tag{13}$$

The model hardens isotropically in accordance with Eq. (7). Integrating Eq. (7) with respect to time results in the second residual expression:

$$R_2\left(\boldsymbol{\sigma}_{n+1}, p_{cT}^{n+1}, \Delta\Lambda\right) = p_{cT}^{n+1}/p_{cT}^{n} - e^{\frac{1+e_0}{\lambda-\kappa}\Delta\varepsilon_{kk}^{p} - \mu\Delta T} \tag{14}$$

where $\varepsilon^{p}{}_{kk}$ is the plastic volumetric strain. The third residual equation imposes the consistency condition to ensure the stress returns back on the yield surface. This can easily be interpreted as the yield value (Eq. (5)):

$$R_3 = y\left(\boldsymbol{\sigma}_{n+1}, p_{cT}^{n+1}\right) \tag{15}$$

These three residual equations are defined by the three unknowns $\boldsymbol{\sigma}_{n+1}$, p_{cT}^{n+1} and $\Delta\Lambda$. At the final state, in which convergence is reached and the residuals are zero, the updated elastic strain and hardening variables are:

$$\boldsymbol{\varepsilon}_{n+1}^{\mathbf{e}} = \boldsymbol{\varepsilon}_n^{e} + \Delta\boldsymbol{\varepsilon} - \Delta\boldsymbol{\varepsilon}^{Therm} - \Delta\boldsymbol{\varepsilon}_{n+1}^{p};\ p_{cT}^{n+1} = p_{cT}^{n} e^{\frac{1+e_0}{\lambda-\kappa}\Delta\varepsilon_{kk}^{p} - \mu\Delta T} \tag{16}$$

The residual equations are required to be minimised and to be solved simultaneously. To minimise the residual incrementally, they are linearised using Taylor's expansion:

$$\begin{aligned}
\ell\mathbf{R}_1 &: \mathbf{R}_1 + (\partial\mathbf{R}_1/\partial\boldsymbol{\sigma}_{n+1})\delta\boldsymbol{\sigma} + \left(\partial\mathbf{R}_1/\partial p_{cT}^{n+1}\right)\delta p_{cT} + (\partial\mathbf{R}_1/\partial\Delta\Lambda)\delta\Lambda = 0 \\
\ell R_2 &: R_2 + (\partial R_2/\partial\boldsymbol{\sigma}_{n+1})\delta\boldsymbol{\sigma} + \left(\partial R_2/\partial p_{cT}^{n+1}\right)\delta p_{cT} + (\partial R_2/\partial\Delta\Lambda)\delta\Lambda = 0 \\
\ell R_3 &: R_3 + (\partial R_3/\partial\boldsymbol{\sigma}_{n+1})\delta\boldsymbol{\sigma} + \left(\partial R_3/\partial p_{cT}^{n+1}\right)\delta p_{cT} + (\partial R_3/\partial\Delta\Lambda)\delta\Lambda = 0
\end{aligned} \tag{17}$$

Equation (17) can be re-written in a compact form as $\mathbf{J}\cdot\mathbf{v} = \mathbf{R}$ where $\mathbf{J}$, $\mathbf{v}$ and $\mathbf{R}$ are the Jacobian matrix, and the increments of unknown and residual vectors, respectively. The unknown increments in each iteration are solved as:

$$\mathbf{v} = \mathbf{J}^{-1}\cdot\mathbf{R} \tag{18}$$

and are added to the previous increment values. The iteration procedure continues until the residual values are within an acceptable tolerance range; the final values represent the values at time $t + \Delta t$ (Eq. (16)).

3.2 Tangent Operator Stiffness Matrix

The momentum equation for finite elements considering materials with elastoplastic behaviour is often solved by a Newton-type iteration solution for finite elements (Eq. (8)). These schemes optimally provide an asymptotic quadratic rate of convergence if the algorithmic tangent operator $\mathbf{D_O}$ is used (Borja 2013). At the end of the iteration process, the residuals become zero and the updated variables are those in Eq. (16). Moving the right hand side of the equations to the left and calling them $\mathbf{T}_1$ and T_2 respectively, and setting T_3 as the yield surface value results in:

$$\begin{aligned}
\mathbf{T}_1 &= \boldsymbol{\varepsilon}_{n+1}^{e} - \left(\boldsymbol{\varepsilon}_n^{e} + \Delta\boldsymbol{\varepsilon} - \Delta\boldsymbol{\varepsilon}^{Therm} - \Delta\boldsymbol{\varepsilon}_{n+1}^{p}\right) = 0 \\
T_2 &= p_{cT}^{n+1} - p_{cT}^{n} e^{\frac{1+e_0}{\lambda-\kappa}\Delta\varepsilon_{kk}^{p} - \mu\Delta T} = 0,\ T_3 = y = 0.
\end{aligned} \tag{19}$$

It should be noted that the above equations have variables of $\boldsymbol{\sigma}_{n+1}$, p_{cT}^{n+1} and $\Delta\Lambda$. Taking the rate of these equations and linearising, yields an equation similar to Eq. (17). Then, an algorithmic solution similar to Eq. (18) can be employed from which the algorithmic tangent operator ($\mathbf{D_O}$) can be extracted:

$$\begin{bmatrix} \delta\boldsymbol{\sigma} \\ \delta p_{cT} \\ \delta\Lambda \end{bmatrix} = \underbrace{\mathbf{J}^{-1}}_{\mathbf{A}} \begin{bmatrix} \delta\boldsymbol{\varepsilon} \\ 0 \\ 0 \end{bmatrix} = \begin{bmatrix} \mathbf{D_O} & \mathbf{A}_{12} & \mathbf{A}_{13} \\ \mathbf{A}_{21} & \mathbf{A}_{22} & \mathbf{A}_{23} \\ \mathbf{A}_{31} & \mathbf{A}_{32} & \mathbf{A}_{33} \end{bmatrix} \begin{bmatrix} \delta\boldsymbol{\varepsilon} \\ 0 \\ 0 \end{bmatrix} \tag{20}$$

4 Numerical Simulations

The shear behaviour of a fully saturated illitic clay under undrained conditions at two temperatures, 22 °C and 75 °C, was investigated by Ghahremannejad (2003). Prior to shearing, the desired temperature was reached (starting from the ambient temperature of 22 °C), and then the samples were hydrostatically consolidated to 400 kPa. Finally,

the samples at a normally consolidated state were sheared under undrained compression to 10%. Figure 1a and b, respectively, show the stress path and shear stress versus shear strain response of the soil at different temperatures. The parameters used for the simulations are summarised in Table 1. The predictions of the model, implemented with the proposed implicit algorithm, are compared with the experimental data in Fig. 1 and are in good agreement, determining the capability of the model to capture the thermomechanical behaviour of the soil.

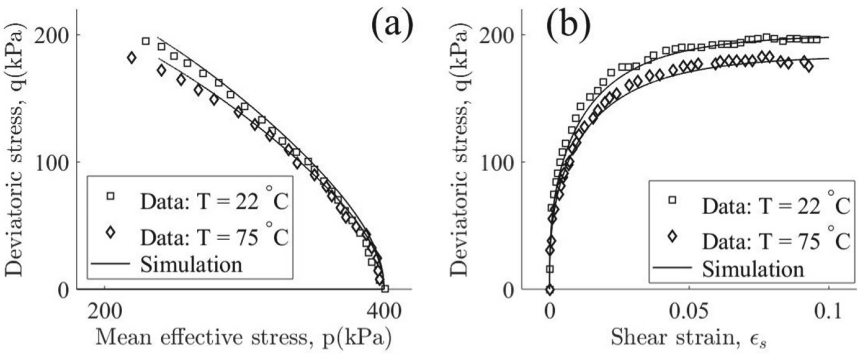

Fig. 1. Comparison of model's predictions with undrained experimental data of Ghahremannejad (2003) at different temperatures; (a) stress path; (b) shear stress vs. shear strain

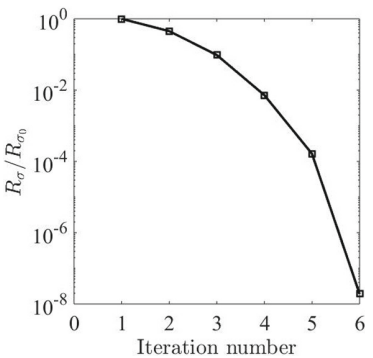

Fig. 2. Normalised residual of the stress by iteration number

Table 1. Summary of model parameters

M_0(−)	λ (−)	K (−)	α (−)	γ (−)	$\overline{\mathbf{G}}$ (kPa)	α^* (1/K)	μ (1/K)	π (1/K)
0.85	0.15	0.03	1.3	0.96	10^4	-3×10^{-5}	9.09×10^{-4}	-1.3×10^{-3}

The performance of the stress integration algorithm is shown by the normalised residual of the stress vector at each iteration (Fig. 2). The residual is $R_\sigma = ((\boldsymbol{\sigma} - \boldsymbol{\sigma}^*) : (\boldsymbol{\sigma} - \boldsymbol{\sigma}^*))^{1/2}$, where $\boldsymbol{\sigma}$ is the estimated stress at each iteration and $\boldsymbol{\sigma}^*$ is the stress at the end of the iteration process. The normalised residual follows a quadratic pattern, i.e., degrades quadratically, showing the effectiveness of the proposed technique.

5 Conclusions

A new implicit stress integration technique for models with nonlinear elasticity, derived by Gibbs energy potential, is proposed, and the tangent operator, to be used for finite elements, is extracted. The stress convergence has been checked and is quadratic. The integration technique has been employed to implement the hyperelasticity-hyperplasticity thermomechanical constitutive model developed by Golchin et al. (2020). The predictions of the model compare well to experimental data available in literature, representing a satisfying performance of the model and integration technique.

Acknowledgements. The support of the Netherlands Organisation for Scientific Research (NWO) through the project number 14698 is acknowledged.

References

Anandarajah, A.: Computational Methods in Elasticity and Plasticity. Springer, New York (2010)

Borja, R.I.: Plasticity, Modeling and Computation. Springer, Heidelberg (2013)

Collins, I.F., Houlsby, G.T.: Application of thermomechanical principles to the modelling of geomaterials. Proc. Math. Phys. Eng. Sci. JSTOR **453**, 1975 (2001)

Coombs, W.M., Crouch, R.S.: Algorithmic issues for three-invariant hyperplastic critical state models. Comput. Methods Appl. Mech. Eng. **200**(25–28), 2297–2318 (2011)

Coombs, W.M., Crouch, R.S., Augarde, C.E.: A unique critical state two-surface hyperplasticity model for fine-grained particulate media. J. Mech. Phys. Solids **61**(1), 175–189 (2013)

Ghahremannejad, B.: Thermo-mechanical behaviour of two reconstituted clays. Ph.D. thesis, University of Sydney (2003)

Golchin, A., Vardon, P.J., Hicks, M.A.: A thermo-mechanical constitutive model for fine-grained soils based on thermodynamics. (2020, Submitted for publication)

Scalet, G., Auricchio, F.: Computational methods for elastoplasticity: an overview of conventional and less-conventional approaches. Arch. Comput. Methods Eng. **25**(3), 545–589 (2018)

Semnani, S.J., White, J.A., Borja, R.I.: Thermoplasticity and strain localization in transversely isotropic materials based on anisotropic critical state plasticity. Int. J. Numer. Anal. Methods Geomech. **40**(18), 2423–2449 (2016)